Research Square

Preprints are preliminary reports that have not undergone peer review.
They should not be considered conclusive, used to inform clinical practice,
or referenced by the media as validated information.

Morphologic Association of the RUAL Classification of Distal Radius Fractures With Ulnar Styloid Base Fractures: A Retrospective Case Series Based on Three-Dimensional Fracture-Line Mapping

Jian Yang
Beijing Jishuitan Hospital, Capital Medical University
Chen Chen
Beijing Jishuitan Hospital, Capital Medical University
Shuai Lu
Beijing Jishuitan Hospital, Capital Medical University
Yejun Zha
Beijing Jishuitan Hospital, Capital Medical University
Xieyuan Jiang
jxytrauma@163.com

Beijing Jishuitan Hospital, Capital Medical University

Research Article

Keywords: distal radius fracture, ulnar styloid fracture, distal radioulnar joint, triangular fibrocartilage complex, three-dimensional fracture-line mapping, classification

Posted Date: November 11th, 2026

DOI: https://doi.org/10.21203/rs.3.rs-11200515/v1

License: This work is licensed under a Creative Commons Attribution 4.0 International License.
Read Full License

Additional Declarations: No competing interests reported.

Title: Morphologic Association of the RUAL Classification of Distal Radius Fractures With Ulnar Styloid Base Fractures: A Retrospective Case Series Based on Three-Dimensional Fracture-Line Mapping

Running title: RUAL Classification and Ulnar Styloid Fracture Morphology

Jian Yang[1,2], Chen Chen[1], Shuai Lu[1] Yejun Zha[1]*, and Xieyuan Jiang[1]*

[1]Department of Orthopaedics and Trauma, Beijing Jishuitan Hospital, Capital Medical University, Beijing, China

[2]Department of Orthopaedics and Trauma, Taihe Hospital, Hubei University of Medicine, Shiyan, Hubei, China

Corresponding author: Yejun Zha, and Xieyuan Jiang

Email address of the corresponding author: jxytrauma@163.com

Abstract

Objective: To develop the RUAL classification based on three-dimensional fracture-line mapping, investigate the association between distinct distal radius fracture morphologies and ulnar styloid base fractures, and assess the potential value of these morphologic patterns as imaging clues to injury of the ulnar-sided osteoligamentous complex.

Methods: We retrospectively included 233 patients with distal radius fractures accompanied by ulnar styloid fractures who were treated at Beijing Jishuitan Hospital between January and December 2023. Preoperative CT data were used for three-dimensional reconstruction, virtual reduction, and fracture-line superimposition. RUAL classification was performed according to the involvement patterns of the sigmoid-notch rim, the scapholunate ridge, and the articular surface. The primary outcome was the distribution of ulnar styloid tip versus base fractures. Categorical variables were analyzed using the Pearson chi-square test; the Fisher–Freeman–Halton exact test was used when expected cell counts were <5, and age was compared using one-way analysis of variance. In an exploratory analysis, types II-A, II-C, and III were combined as a morphologic high-risk group, whereas types I and II-B were combined as a low/intermediate-risk group. Odds ratios (ORs) and 95% confidence intervals (CIs) were calculated. In addition, 80 imaging studies were randomly selected and independently interpreted twice, 4 weeks apart, by two experienced musculoskeletal attending physicians who had undergone standardized training. Interobserver and intraobserver reliability were assessed using unweighted Cohen's kappa with 95% CIs.

Results: RUAL type I was identified in 100 patients (42.9%), type II in 115 (49.4%), and type III in 18 (7.7%). Among type II fractures, 16 were type II-A, 87 were type II-B, and 12 were type II-C. The distribution of ulnar styloid fracture location did not differ significantly across the six subtypes (χ^2=5.071, P=0.407) or among the three major RUAL types (χ^2=0.533, P=0.766). After exploratory pooling, ulnar styloid base fractures were present in 26 of 46 patients (56.5%) in the high-risk group and 74 of 187 patients (39.6%) in the low/intermediate-risk group. This difference was statistically significant (χ^2=4.329, P=0.037), with an OR of 1.99 for base fracture in the high-risk group relative to the low/intermediate-risk group (95% CI, 1.03–3.81; Fisher's exact test, P=0.046). For reliability, interobserver κ values were 0.631 (95% CI, 0.496–0.765) and 0.570 (95% CI, 0.424–0.717) in the two reading rounds, respectively; intraobserver κ values were 0.909 (95% CI, 0.831–0.986) and 0.826 (95% CI, 0.726–0.927) for the two observers, respectively (all P<0.001).

Conclusion: Overall comparisons across the three major RUAL types and six subtypes did not demonstrate a significant difference in ulnar styloid fracture location. However, exploratory risk grouping suggested that volar or combined volar–dorsal sigmoid-notch rim disruption and a central sagittal split were associated with enrichment of ulnar styloid base fractures. These morphologic patterns may therefore serve as imaging warning signs prompting further assessment of the triangular fibrocartilage complex (TFCC) and distal radioulnar joint (DRUJ) stability, but they should not be used to directly diagnose a deep TFCC tear or to determine whether the ulnar styloid should be fixed.

Keywords: distal radius fracture; ulnar styloid fracture; distal radioulnar joint; triangular fibrocartilage complex; three-dimensional fracture-line mapping; classification

Introduction

Distal radius fractures are among the most common upper-extremity fractures, and approximately 50% are accompanied by an ipsilateral ulnar styloid fracture [1,2]. Ulnar styloid base fractures are often associated with tears of the deep fibers of the triangular fibrocartilage complex (TFCC) and may result in distal radioulnar joint (DRUJ) instability [3,4], although their clinical relevance and implications for treatment remain controversial. Several studies have reported that a concomitant ulnar styloid fracture has little or no effect on wrist functional recovery [5–7], particularly when the DRUJ is

stable after fixation of the radius [8]. Conversely, other evidence suggests a higher incidence of postoperative ulnar-sided wrist pain in patients with base fractures [9,10]. These conflicting findings highlight the limitations of conventional classifications and the need for more precise morphologic tools for risk stratification.

DRUJ stability depends in part on the TFCC attachment at the base of the ulnar styloid [11,12]. Avulsion fractures at the styloid base may indicate failure of the deep TFCC fibers [4]. However, the quantitative relationship between specific distal radius fracture morphologies, such as sigmoid-notch rim fractures, and ulnar styloid base fractures has not been systematically characterized [13]. Previous studies have largely focused on global displacement parameters [14] or biomechanical behavior [15], rather than on detailed correspondence between patterns of structural disruption. We therefore developed a new classification for distal radius fractures with concomitant ulnar styloid fractures—the RUAL (Radioulnar Articular Coupling) classification—by comprehensively evaluating involvement of the scaphoid and lunate fossae, the volar and dorsal rims, patterns of sigmoid-notch injury, sagittal splitting along the scapholunate ridge, and the precise anatomic location of the ulnar styloid fracture (tip vs base). We further analyzed the association between specific distal radius fragment patterns and the anatomic location of the ulnar styloid fracture.

Materials and Methods

Study Design and Patient Selection

This single-center retrospective case-series study consecutively screened patients treated at Beijing Jishuitan Hospital from January through December 2023. Because all eligible cases within the prespecified study period were included, no a priori sample-size calculation was performed. The inclusion criteria were: (1) an acute, closed, unstable distal radius fracture; (2) complete preoperative high-resolution multidetector CT data suitable for three-dimensional reconstruction; and (3) a concomitant ipsilateral ulnar styloid fracture. The exclusion criteria were: (1) skeletal immaturity; (2) pre-existing wrist deformity; (3) severe metabolic bone disease; and (4) CT image quality insufficient for three-dimensional reconstruction. A total of 233 patients were ultimately included. Age, sex, and mechanism of injury were extracted from the electronic medical record.

Three-Dimensional Reconstruction, Standardization, and Fracture-Line Mapping

Raw DICOM data were imported into Mimics Medical 21.0 (Materialise, Leuven, Belgium) for segmentation, three-dimensional reconstruction, and virtual anatomic reduction. STL files were then exported to 3-matic (Materialise, Leuven, Belgium), where fracture lines were traced. A CT scan of the right wrist of an adult woman without wrist pathology was selected to create the standard template. To standardize orientation, the articular-surface view was defined with the dorsal side superiorly, the volar side inferiorly, the radial side to the left, and the ulnar side to the right; left-wrist data were mirrored to the right. Two experienced musculoskeletal imaging physicians independently identified the fracture lines, and confirmed fracture lines were projected onto the standard template to generate fracture-line distribution maps and heat maps (Fig. 1).

RUAL Morphologic Variables and Classification

For each case, involvement of the scaphoid fossa, central lunate fossa, volar rim, dorsal rim, and sigmoid notch was recorded, as was the presence of a sagittal split along the scapholunate ridge (Fig. 2). Ulnar styloid fractures were categorized as tip or base fractures. This anatomy-oriented system was termed the RUAL (Radioulnar Articular Coupling) classification. RUAL type I was defined as a column-stable pattern in which the key volar and dorsal rims of the sigmoid notch remained continuous, including type I-Ext (extra-articular) and type I-Int (simple intra-articular fracture). Type II was defined as a sigmoid-notch rim disruption pattern and included type II-A (volar rim), type II-B (dorsal rim), and type II-C (combined volar and dorsal rim disruption or complete sigmoid-notch comminution). Type III was defined as a central sagittal split along the scapholunate ridge.

Outcome Measures and Exploratory Risk Grouping

The primary morphologic outcome was the distribution of ulnar styloid tip and base fractures across RUAL types. A base fracture was regarded as an imaging marker of increased risk for involvement of the deep TFCC insertion, rather than as a surrogate diagnosis of complete TFCC rupture or DRUJ instability. To explore the clustering effect of disruption to key stabilizing structures of the sigmoid notch, an exploratory pooled analysis was performed: types II-A, II-C, and III were defined as the morphologic high-risk group, whereas type I and type II-B were defined as the

low/intermediate-risk group. This pooled analysis was intended for hypothesis generation and was not treated as an externally validated clinical risk score.

Reliability Assessment

Eighty patients with complete preoperative CT and three-dimensional reconstruction data were randomly selected from the 233-patient cohort for assessment of RUAL classification reliability. Before formal image interpretation, two experienced attending orthopedic trauma physicians underwent standardized training to familiarize them with the RUAL criteria and the imaging features defining each subtype. After training, the two observers independently classified the 80 imaging studies while blinded to each other's assessments. Four weeks after the first reading, the studies were randomly reordered, and both observers repeated the classifications independently without access to their initial results.

Statistical Analysis

Statistical analyses were performed using SPSS version 26.0 (IBM Corp., Armonk, NY, USA), and all aggregate frequencies were independently cross-checked. Normally distributed continuous variables are presented as mean ± standard deviation and were compared among three groups using one-way analysis of variance. Categorical variables are presented as counts and percentages and were analyzed using the Pearson chi-square test when all expected cell counts were ≥5; otherwise, a two-sided Fisher–Freeman–Halton exact test was used. For the exploratory 2×2 contingency table, both the Pearson chi-square test and Fisher's exact test were reported, together with the OR for ulnar styloid base fracture and its 95% CI. All tests were two-sided, with $\alpha=0.05$. Because the pooled risk analysis was exploratory, P values were interpreted at the nominal level without adjustment for multiple comparisons.

The six RUAL subtypes (I-Ext, I-Int, II-A, II-B, II-C, and III) were treated as nominal categorical variables. Interobserver and intraobserver diagnostic reliability were evaluated using unweighted Cohen's κ, with raw agreement rates and 95% CIs also reported. Interobserver κ was calculated separately for each of the two reading rounds, and intraobserver κ was calculated by comparing each observer's first and second readings. The 95% CIs for κ were calculated using large-sample asymptotic standard errors.

Because the available dataset contained only aggregate frequencies and did not include patient-level covariates such as fragment displacement, sigmoid-notch step-off,

or ulnar variance, multivariable logistic regression was not performed. The association between exploratory risk grouping and ulnar styloid base fracture is therefore reported only as an unadjusted OR with a 95% CI. This analysis was intended to generate a morphologic hypothesis rather than to establish an independent prediction after adjustment for confounding variables.

Ethics Approval

This study was approved by the Ethics Committee of Beijing Jishuitan Hospital (approval No. K2026241-01). Written informed consent to participate was obtained from all participants included in the study. The study was conducted in accordance with the Declaration of Helsinki and applicable institutional and national regulations.

Results

Baseline Characteristics

Among the 233 patients, 91 (39.1%) were men and 142 (60.9%) were women, with a mean age of 59.2±11.8 years. Low-energy injuries occurred in 205 patients (88.0%) and high-energy injuries in 28 (12.0%). There were no statistically significant differences among RUAL types I, II, and III in sex, age, or mechanism of injury (all $P>0.05$; Table 1). The minimum expected cell count in the contingency table for mechanism of injury was 2.16; therefore, the Fisher–Freeman–Halton exact test was used.

Distribution and Morphologic Characteristics of RUAL Types

RUAL type I was identified in 100 patients (42.9%), including 34 with type I-Ext and 66 with type I-Int. Type II was identified in 115 patients (49.4%), including 16 with type II-A, 87 with type II-B, and 12 with type II-C; the total number of type II cases was reconfirmed as 115. Type III was identified in 18 patients (7.7%). The distribution of ulnar styloid tip and base fractures across subtypes is shown in Table 2 and Fig. 3. The overall comparison among the six subtypes was not statistically significant ($\chi^2=5.071$, $P=0.407$).

The defining feature of type I was continuity of the volar and dorsal rims of the sigmoid notch. The rates of ulnar styloid base fracture were 41.2% for type I-Ext and 40.9% for type I-Int (Figs. 4 and 5). Type II was characterized by sigmoid-notch rim involvement: type II-A showed separation of the volar rim and had a base-fracture rate of 62.5%; type II-B predominantly involved the dorsal rim and had a rate of 37.9%; and

type II-C involved both volar and dorsal rims and had a rate of 58.3% (Figs. 6–8). Type III showed a central sagittal split along the scapholunate ridge, with a base-fracture rate of 50.0% (Fig. 9). These percentages describe the distribution within the present sample. Given the small number of cases in several individual subtypes, they should not be interpreted as evidence of independent predictive performance.

Association Between RUAL Type and Ulnar Styloid Fracture Location

The rates of ulnar styloid base fracture were 41.0%, 43.5%, and 50.0% for types I, II, and III, respectively, with no statistically significant difference among the three groups (χ^2=0.533, P=0.766; Table 3). Thus, the overall comparison of the three major RUAL types did not support an association between major RUAL type and ulnar styloid fracture location.

In the exploratory pooled analysis, the base-fracture rate was 56.5% (26/46) in the high-risk group and 39.6% (74/187) in the low/intermediate-risk group, a statistically significant difference (χ^2=4.329, P=0.037; two-sided Fisher's exact test, P=0.046). Using the low/intermediate-risk group as the reference, the high-risk group had an OR of 1.99 for base fracture (95% CI, 1.03–3.81), a risk ratio of 1.43 (95% CI, 1.05–1.95), and an absolute risk difference of 16.9 percentage points (95% CI, 1.0–32.9 percentage points) (Table 4, Fig. 10). The confidence intervals for these effect estimates were relatively wide and the P values were close to 0.05, indicating limited precision.

Reliability Assessment and Unadjusted Analysis

All 80 randomly selected imaging studies underwent two independent reading rounds with no missing data. In the first round, the two observers agreed completely in 59 cases, corresponding to a raw agreement of 73.8% and κ=0.631 (95% CI, 0.496–0.765; Z=10.666; P<0.001). In the second round, complete agreement was achieved in 56 cases, with a raw agreement of 70.0% and κ=0.570 (95% CI, 0.424–0.717; Z=9.401; P<0.001). Observer 1 produced identical classifications in 75 cases across the two rounds, yielding a raw intraobserver agreement of 93.8% and κ=0.909 (95% CI, 0.831–0.986; Z=14.498; P<0.001). Observer 2 produced identical classifications in 70 cases, yielding a raw intraobserver agreement of 87.5% and κ=0.826 (95% CI, 0.726–0.927; Z=14.018; P<0.001) (Table 5).

Because patient-level covariates suitable for adjustment were unavailable, multivariable logistic regression was not performed. The association between the high-risk group and ulnar styloid base fracture shown in Table 4 is therefore unadjusted:

OR=1.99 (95% CI, 1.03–3.81), Pearson χ^2 P=0.037, and two-sided Fisher's exact P=0.046. This finding should be interpreted only as an exploratory signal of morphologic enrichment.

Discussion

Principal Findings

Using preoperative three-dimensional CT data from 233 patients with distal radius fractures accompanied by ulnar styloid fractures, we developed the RUAL morphologic classification based primarily on continuity of the volar and dorsal rims of the sigmoid notch and the presence of a central sagittal split along the scapholunate ridge. Overall comparisons across the six subtypes and the three major types did not demonstrate a significant difference in the distribution of ulnar styloid tip versus base fractures, indicating that the RUAL classification cannot currently be regarded as a deterministic classifier of ulnar styloid fracture location. In the exploratory pooled analysis, however, the base-fracture rate was higher in the high-risk group comprising types II-A, II-C, and III than in the low/intermediate-risk group (56.5% vs 39.6%), with an unadjusted OR of 1.99 (95% CI, 1.03–3.81). Because this analysis was not adjusted for multiple comparisons, was not externally validated, and did not account for potential confounders, the finding should be interpreted as a signal of morphologic enrichment in specific distal-radius patterns rather than as a validated predictive model, a surrogate diagnosis of deep TFCC rupture, or an indication for ulnar styloid fixation.

Morphologic Value of the RUAL Classification

The RUAL classification may complement conventional systems by providing a more detailed description of the osseous components of the DRUJ. Classifications such as AO/OTA, Frykman, and Fernandez primarily summarize extra-articular versus intra-articular involvement, direction of displacement, degree of comminution, or presumed injury mechanism and therefore do not fully capture the three-dimensional distinctions among disruption of the volar sigmoid-notch rim, dorsal rim, both rims, and a central sagittal split. Previous studies have shown that three-dimensional fracture-line mapping can identify high-frequency fracture trajectories, anatomic weak zones, and morphologic heterogeneity within a single conventional fracture category that may be difficult to appreciate on standard two-dimensional imaging [16–18]. On this basis, the RUAL classification places radial-sided sigmoid-notch injury and ulnar-sided osteoligamentous injury within the same DRUJ anatomic framework. At present,

however, its principal value lies in standardized morphologic description and hypothesis generation; its clinical utility requires further assessment of reliability, external validation, and associations with clinical outcomes.

Anatomic Basis of High-Risk Morphologies

DRUJ stability is maintained by the osseous congruity of the sigmoid notch and ulnar head together with the TFCC, joint capsule, and distal interosseous membrane structures. The deep fibers of the distal radioulnar ligaments insert into the ulnar fovea and are important restraints to dorsal and volar translation of the ulnar head. Arthroscopic studies have shown that ulnar styloid base fractures are more frequently associated with TFCC type 1B injury [19], while cadaveric work has demonstrated that base osteotomy involving the ulnar fovea increases forearm pronation and supination [20]. Residual distal radioulnar ligament fibers may nevertheless preserve some stability, and a base fracture does not necessarily imply complete instability [21]. In the present study, type II-A may reflect disruption of the volar osseous restraint, type II-C may indicate more extensive destruction of the sigmoid-notch containment surface, and type III may divide the distal radial articular surface into relatively independent radial and ulnar units. These interpretations remain mechanistic hypotheses. In the absence of arthroscopy, standardized MRI, and intraoperative stability data, the present study cannot establish a causal relationship between RUAL morphology and deep TFCC rupture or DRUJ instability.

Negative Overall Findings and the Exploratory Signal

The absence of a significant overall difference across the six subtypes and three major types is not inconsistent with the statistical signal observed after pooling selected morphologies. The overall tests evaluated distributional differences across all categories, whereas the exploratory pooled analysis tested a prespecified contrast based on disruption of key stabilizing structures of the sigmoid notch. Heterogeneity within type II may have diluted the overall effect: base-fracture rates were 62.5%, 37.9%, and 58.3% for types II-A, II-B, and II-C, respectively, and type II-B—the largest subgroup—did not show the same directional pattern as types II-A and II-C. Previous studies suggest that DRUJ instability is more closely related to complete TFCC foveal tears and increased fracture-fragment gap than to the ulnar styloid fracture location alone [22]. Accordingly, the type II-B finding should not be interpreted as evidence that dorsal-rim involvement is protective. Future studies should consider the direction of

involvement together with fragment size, displacement and rotation, sigmoid-notch step-off, and soft-tissue status. Osseous morphology, joint stability, and clinical function should also be evaluated as distinct but related outcome levels [23].

Clinical Implications and Limits of Application

The most appropriate current clinical use of a high-risk RUAL morphology is to heighten awareness of possible combined DRUJ injury and to prompt targeted assessment, rather than to directly determine whether the ulnar styloid should be fixed. When preoperative CT demonstrates type II-A, II-C, or III morphology, the ulnar styloid fragment should be further assessed for involvement of the ulnar fovea, as well as for fragment size, rotation, and displacement; sigmoid-notch step-off, gap, comminution, radial shortening, and ulnar variance should also be evaluated. After reduction and fixation of the distal radius, DRUJ congruity and stability should still be examined in neutral rotation, pronation, and supination. In the presence of persistent ulnar-sided pain, obvious clicking, or an abnormal ballottement test, MRI, ultrasonography, dynamic CT, or arthroscopy may be considered for further evaluation of the TFCC. Existing clinical studies have not shown that the presence or fixation of an ulnar styloid fracture consistently improves long-term function or DRUJ stability [24–27], and sigmoid-notch involvement may increase radiographic osteoarthritis without corresponding differences in pain or function [28]. Thus, a high-risk morphology cannot substitute for assessment of residual instability, and a low/intermediate-risk morphology cannot exclude TFCC injury. This interpretation is consistent with current guideline principles that treatment should be individualized according to fracture morphology, functional demands, and clinical stability [29,30].

Strengths and Limitations

This study used a standardized workflow for three-dimensional reconstruction, virtual reduction, and template projection to characterize sigmoid-notch rim and central split morphologies in a relatively large consecutive case series. We reported the negative overall findings together with exploratory effect estimates and 95% CIs. In the reliability analysis of 80 randomly selected cases, interobserver κ values were 0.631 and 0.570 across the two rounds, while intraobserver κ values were 0.909 and 0.826 for the two observers, indicating moderate interobserver agreement and high intraobserver stability. The principal limitations are the single-center retrospective design and inclusion only of patients with a concomitant ulnar styloid fracture; the relatively small

high-risk group; the absence of adjustment for multiple comparisons or confounding variables and the lack of external validation; the use of ulnar styloid base fracture only as an indirect marker of deep TFCC insertional involvement, without arthroscopic, MRI, or intraoperative DRUJ stability reference standards; operator dependence in virtual reduction, template registration, and fracture-line tracing; and the lack of follow-up outcomes for pain, function, grip strength, stability, or reoperation. Future multicenter prospective studies should prespecify the classification rules and high-risk grouping, include the full spectrum of distal radius fractures, and assess incremental value using independent reliability testing, multivariable models, soft-tissue or stability reference standards, and external validation.

Conclusion

Among 233 patients with distal radius fractures accompanied by ulnar styloid fractures, overall comparisons across the six RUAL subtypes and three major types did not show a significant difference in the distribution of ulnar styloid tip versus base fractures. Exploratory pooled analysis suggested relative enrichment of ulnar styloid base fractures in fractures with volar or combined volar–dorsal sigmoid-notch rim disruption or a central sagittal split (OR=1.99; 95% CI, 1.03–3.81). This signal supports more careful assessment of the TFCC and DRUJ stability when these morphologies are present, but it is not sufficient to replace direct soft-tissue assessment or to serve as an independent indication for routine ulnar styloid fixation.

Abbreviations

CI, confidence interval; CT, computed tomography; DASH, Disabilities of the Arm, Shoulder and Hand; DICOM, Digital Imaging and Communications in Medicine; DRUJ, distal radioulnar joint; OR, odds ratio; PRWE, Patient-Rated Wrist Evaluation; RUAL, Radioulnar Articular Coupling classification; STL, stereolithography file; TFCC, triangular fibrocartilage complex.

Declarations

Ethics Approval and Consent to Participate

This study was approved by the Ethics Committee of Beijing Jishuitan Hospital (ethics approval reference number: K2026241-01; date of approval: June 29, 2026). Written informed consent to participate was obtained from all participants included in

the study. All study procedures were conducted in accordance with the Declaration of Helsinki and applicable institutional and national regulations.

Consent for Publication

The figures in this manuscript consist of standardized three-dimensional fracture-line maps, bone models, and aggregate statistical graphics and do not display names, medical record numbers, facial images, or other directly identifying information. Whether consent for publication may be stated as "not applicable" should be confirmed by the authors in accordance with the target journal's requirements and the ethics approval.

Availability of Data and Materials

The current manuscript does not provide a public repository, permanent link, or information on approval for data sharing. Because the study involves patient CT images and medical-record data, the corresponding author should determine the appropriate data-availability statement in accordance with the ethics approval, the scope of informed consent or waiver, and institutional data-governance policies. The data should not be described as publicly or unconditionally available until these matters have been verified.

Author Contributions

Jian Yang contributed to study conception, methodology, data curation, formal analysis, visualization, and manuscript preparation. Yejun Zha contributed to formal analysis, supervision, funding acquisition, visualization, project administration, resource provision, and manuscript preparation. Chen Chen contributed to study conception, methodology, formal analysis, visualization, supervision, and resource provision. Shuai Lu contributed to data curation, validation, formal analysis, and visualization. Xieyuan Jiang contributed to supervision, funding acquisition, visualization, project administration, and resource provision. All authors read and approved the final manuscript.

Competing Interests

The materials currently available do not contain declarations of competing interests from all authors. Each author should complete the required disclosure, after which a consolidated statement should be prepared. The absence of competing interests should not be inferred from the study data.

Acknowledgements

The available materials do not indicate whether any contributors who do not meet authorship criteria should be acknowledged. This should be confirmed by all authors; “not applicable” should not be stated without such confirmation.

Funding

This study was supported by the Capital’s Funds for Health Improvement and Research (grant No. SF 2026-1Q-1062) and the Hubei Provincial Natural Science Foundation (grant No. 2026AFC1440).

References

[1] KOKUBU Y, OBI A, KIMURA Y, et al. Hip bone density is associated with concomitant distal ulna fracture in the setting of distal radius fracture.[J/OL]. Osteoporosis international : a journal established as result of cooperation between the European Foundation for Osteoporosis and the National Osteoporosis Foundation of the USA, 2026. DOI:10.1007/s00198-026-07984-w.

[2] KIM J K, KIM J O, KOH Y D. Management of Distal Ulnar Fracture Combined with Distal Radius Fracture.[J/OL]. The journal of hand surgery Asian-Pacific volume, 2016, 21(2): 155-160. DOI:10.1142/S2424835516400075.

[3] KIM K W, LEE C H, CHOI J H, et al. Distal radius fracture with concomitant ulnar styloid fracture: does distal radioulnar joint stability depend on the location of the ulnar styloid fracture?[J/OL]. Archives of orthopaedic and trauma surgery, 2023, 143(2): 839-845. DOI:10.1007/s00402-021-04199-y.

[4] HUANG H K, WU C H, WANG J P. Distal Radioulnar Joint Instability in Distal Radius Fracture.[J/OL]. The journal of hand surgery Asian-Pacific volume, 2025, 30(6): 571-581. DOI:10.1142/S2424835525400090.

[5] LEE J I, PARK J W, PARK K C, et al. Predictors for nonunion of unrepaired ulnar styloid fracture associated with distal radius fractures in patients treated with volar locking plate fixation and their effect on functional outcomes.[J/OL]. Orthopaedics & traumatology, surgery & research : OTSR, 2022, 108(5): 103322. DOI:10.1016/j.otsr.2022.103322.

[6] SAWADA H, SHINOHARA T, NATSUME T, et al. Clinical effects of internal fixation for ulnar styloid fractures associated with distal radius fractures: A matched case-control study.[J/OL]. Journal of orthopaedic science : official journal of the Japanese Orthopaedic Association, 2016, 21(6): 745-748. DOI:10.1016/j.jos.2016.06.010.

[7] MULDERS M A M, SNETHLAGE L J F, KEIZER R J O de M, et al. Functional outcomes of distal radius fractures with and without ulnar styloid fractures: a meta-analysis.[J/OL]. The Journal of hand surgery, European volume, 2018, 43(2): 150-157. DOI:10.1177/1753193417730323.

[8] LI S, WANG H, SU B, et al. Impact of Ulnar Styloid Fractures on the Treatment Effect of Distal Radius Fractures with Volar Plate Fixation: A Case Control Study.[J/OL]. Indian journal of orthopaedics, 2020, 54(1): 75-82. DOI:10.1007/s43465-019-00016-2.

[9] OZBEN H, ULUDAĞ S, ATAKER Y, et al. Distal radius fractures: What are the effects of ulnar styloid fracture and face-toface rehabilitation on the functional outcome?[J/OL]. Acta orthopaedica et traumatologica turcica, 2023, 57(6): 361-365. DOI:10.5152/j.aott.2023.21245.

[10] ZHANG P, JIA B, CHEN X K, et al. [Effects of ulnar styloid and sigmoid notch fractures on postoperative wrist function of patients with distal radius fracture].[J/OL]. Beijing da xue xue bao. Yi xue ban = Journal of Peking University. Health sciences, 2020, 52(3): 578-581. DOI:10.19723/j.issn.1671-167X.2020.03.027.

[11] TSAI P C, PAKSIMA N. The distal radioulnar joint.[J]. Bulletin of the NYU hospital for joint diseases, 2009, 67(1): 90-96.

[12] MAULER F, BOUDABBOUS S, BEAULIEU J Y. Midsectional Magnetic Resonance Imaging Analysis of the Sigmoid Notch of the Distal Radioulnar Joint.[J/OL]. Journal of wrist surgery, 2023, 12(2): 170-176. DOI:10.1055/s-0042-1750874.

[13] COLE D W, ELSAIDI G A, KUZMA K R, et al. Distal radioulnar joint instability in distal radius fractures: the role of sigmoid notch and triangular fibrocartilage complex revisited.[J/OL]. Injury, 2006, 37(3): 252-258. DOI:10.1016/j.injury.2005.08.019.

[14] FUJITANI R, OMOKAWA S, AKAHANE M, et al. Predictors of distal radioulnar joint instability in distal radius fractures.[J/OL]. The Journal of hand surgery, 2011, 36(12): 1919-1925. DOI:10.1016/j.jhsa.2011.09.004.

[15] NISHIWAKI M, WELSH M, GAMMON B, et al. Distal radioulnar joint kinematics in simulated dorsally angulated distal radius fractures.[J/OL]. The Journal of hand surgery, 2014, 39(4): 656-663. DOI:10.1016/j.jhsa.2014.01.013.

[16] Li S, Zhang YQ, Wang GH, Li K, Wang J, Ni M. Melone's concept revisited in comminuted distal radius fractures: the three-dimensional CT mapping. J Orthop Surg Res. 2020;15(1):222. doi:10.1186/s13018-020-01739-x.

[17] Yao P, Gong M, Shan L, Wang D, He Y, Wang H, et al. Tibial plateau fractures: three dimensional fracture mapping and morphologic measurements. Int Orthop. 2022;46(9):2153-2163. doi:10.1007/s00264-022-05434-w.

[18] Chen S, Zheng Z, Guo J, Hong S, Zhou W, Xie J, et al. Three-dimensional computed tomography mapping techniques in the morphometric analysis of AO/OTA 33A and 33C distal femoral fractures: a retrospective single-center study. Front Bioeng Biotechnol. 2023;11:1162214. doi:10.3389/fbioe.2023.1162214.

[19] Tomori Y, Nanno M, Takai S. The presence and the location of an ulnar styloid fracture associated with distal radius fracture predict the presence of triangular fibrocartilage complex 1B injury. Arthroscopy. 2020;36(10):2674-2680. doi:10.1016/j.arthro.2020.05.025.

[20] Pidgeon TS, Crisco JJ, Waryasz GR, Moore DC, DaSilva MF. Ulnar styloid base fractures cause distal radioulnar joint instability in a cadaveric model. Hand (N Y). 2018;13(1):65-73. doi:10.1177/1558944716685830.

[21] Maniglio M, Park IJ, Kuenzler M, Zumstein MA, McGarry MH, Lee TQ. Residual stability of the distal radioulnar joint following ulnar styloid fracture: influence of the remnant distal radioulnar ligaments. J Hand Surg Eur Vol. 2022;47(9):944-951. doi:10.1177/17531934221088508.

[22] Kim KW, Lee CH, Choi JH, Ahn JM, Gong HS. Distal radius fracture with concomitant ulnar styloid fracture: does distal radioulnar joint stability depend on the location of the ulnar styloid fracture? Arch Orthop Trauma Surg. 2023;143(2):839-845. doi:10.1007/s00402-021-04199-y.

[23] Haugstvedt JR, Langer MF, Berger RA. Distal radioulnar joint: functional anatomy, including pathomechanics. J Hand Surg Eur Vol. 2017;42(4):338-345. doi:10.1177/1753193417693170.

[24] Mulders MAM, Fuhri Snethlage LJ, de Muinck Keizer RJO, Goslings JC, Schep NWL. Functional outcomes of distal radius fractures with and without ulnar styloid fractures: a meta-analysis. J Hand Surg Eur Vol. 2018;43(2):150-157. doi:10.1177/1753193417730323.

[25] Okoli M, Silverman M, Abboudi J, Jones C, Kirkpatrick W, Liss F, et al. Radiographic healing and functional outcomes of untreated ulnar styloid fractures following volar plate fixation of distal radius fractures: a prospective analysis. Hand (N Y). 2021;16(3):332-337. doi:10.1177/1558944719855445.

[26] Kumar P, Dadra A, Rajnish RK, Sharma S, Patel S, Dhillon MS, et al. Ipsilateral fractures of the ulnar styloid with distal radius fractures; to fix or not? A systematic review and meta-analysis. J Clin Orthop Trauma. 2024;55:102519. doi:10.1016/j.jcot.2024.102519.

[27] Xiao AX, Graf AR, Dawes A, Daley C, Wagner ER, Gottschalk MB. Management of acute distal radioulnar joint instability following a distal radius fracture: a systematic review and meta-analysis. J Hand Surg Glob Online. 2021;3(3):133-138. doi:10.1016/j.jhsg.2021.02.005.

[28] Kim YS, Lim JH, Kim MS. The impact of sigmoid notch involvement on the outcomes of distal radius fractures: radiological and clinical assessments after a minimum of 5 years of follow-up. Clin Orthop Surg. 2025;17(4):568-574. doi:10.4055/cios24102.

[29] Kamal RN, Shapiro LM. American Academy of Orthopaedic Surgeons/American Society for Surgery of the Hand clinical practice guideline summary:

management of distal radius fractures. J Am Acad Orthop Surg. 2022;30(4):e480-e486. doi:10.5435/JAAOS-D-21-00719.

[30] Shapiro LM, Kamal RN; Management of Distal Radius Fractures Work Group, et al. Distal radius fracture clinical practice guidelines-updates and clinical implications. J Hand Surg Am. 2021;46(9):807-811. doi:10.1016/j.jhsa.2021.07.014.

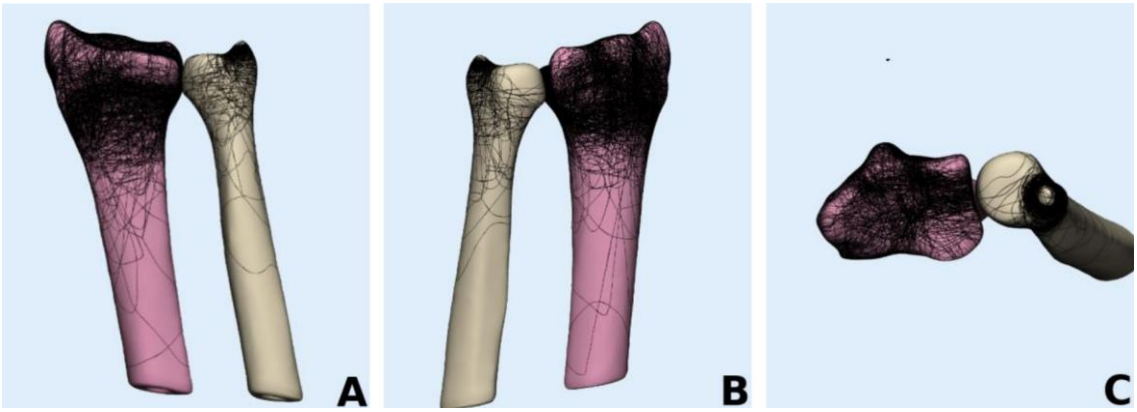


Figure 1. Fracture-line distribution map of 233 distal radius fractures accompanied by ulnar styloid fractures. (A) Volar view; (B) dorsal view; (C) articular-surface view.

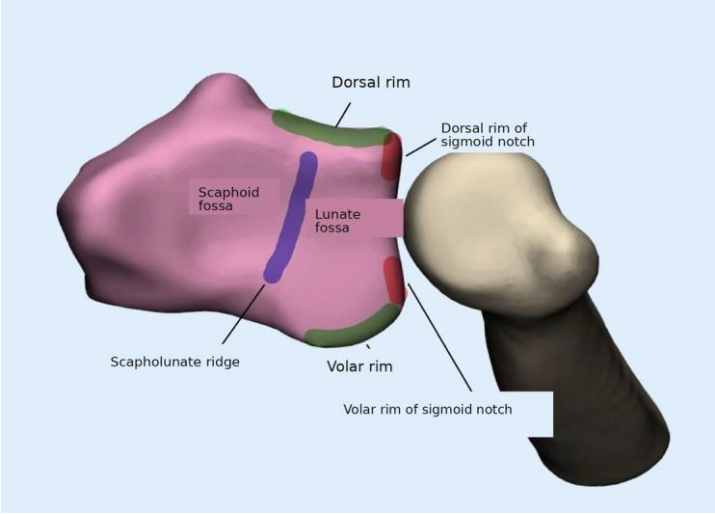


Figure 2. Schematic illustration of the recorded anatomic landmarks on the distal radial articular surface.

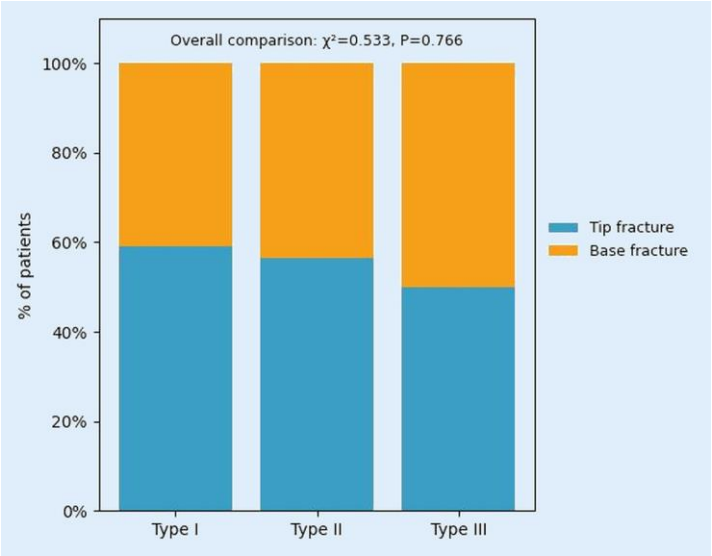


Figure 3. Distribution of ulnar styloid tip and base fractures across the three major RUAL types.

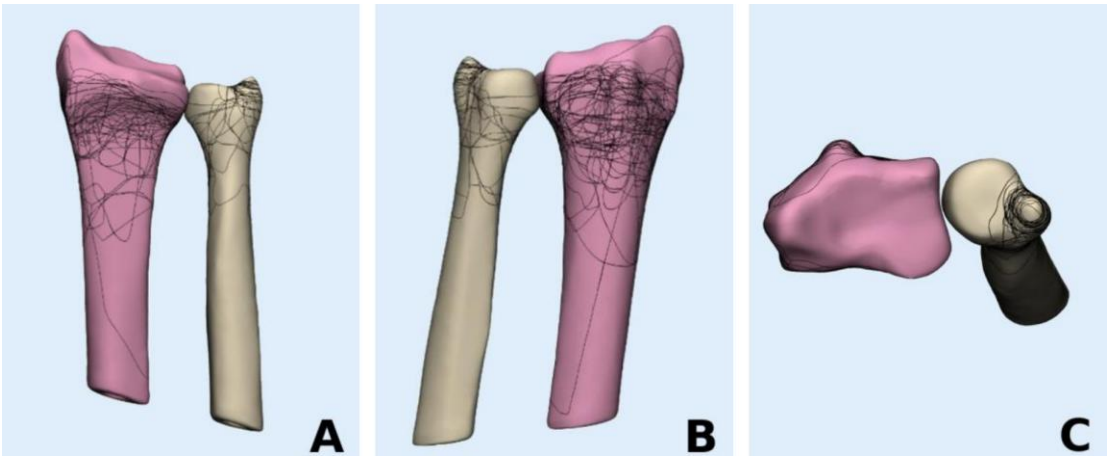


Figure 4. Fracture-line distribution map of 34 RUAL type I-Ext fractures. (A) Volar view; (B) dorsal view; (C) articular-surface view.

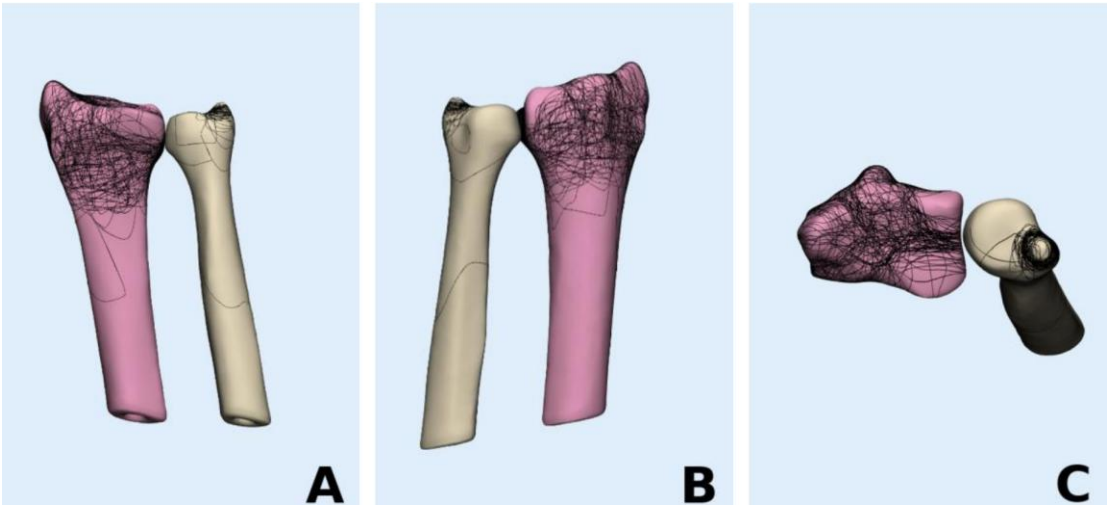


Figure 5. Fracture-line distribution map of 66 RUAL type I-Int fractures. (A) Volar view; (B) dorsal view; (C) articular-surface view.

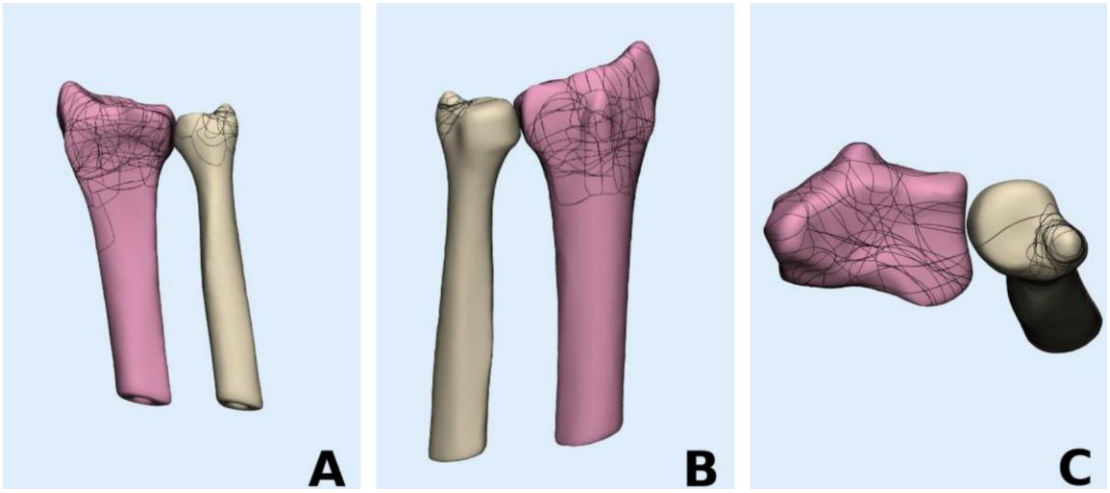


Figure 6. Fracture-line distribution map of 16 RUAL type II-A fractures. (A) Volar view; (B) dorsal view; (C) articular-surface view.

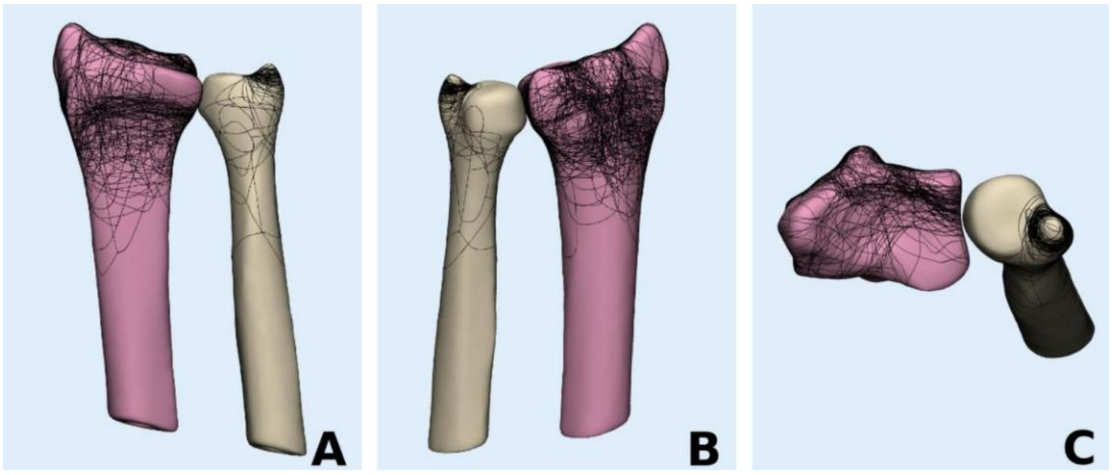


Figure 7. Fracture-line distribution map of 87 RUAL type II-B fractures. (A) Volar view; (B) dorsal view; (C) articular-surface view.

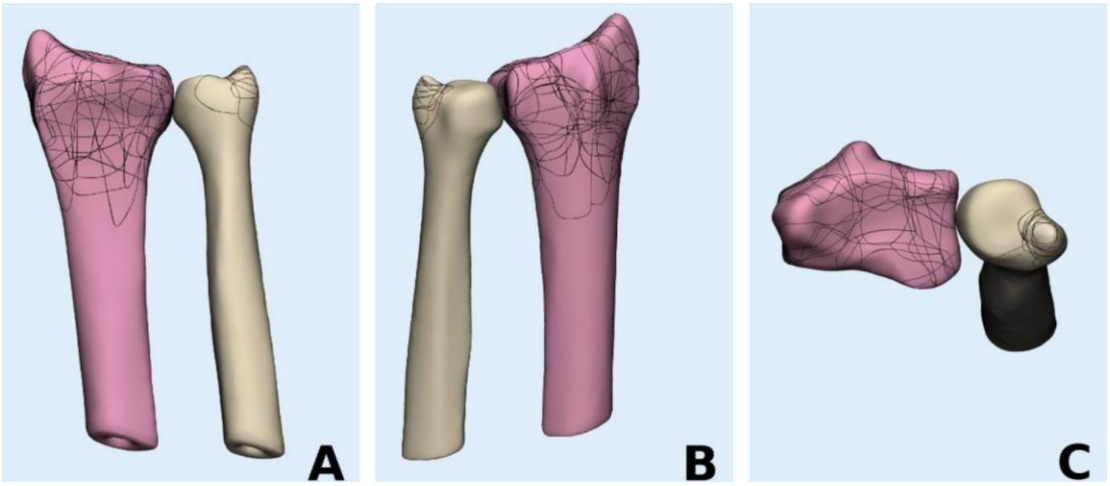


Figure 8. Fracture-line distribution map of 12 RUAL type II-C fractures. (A) Volar view; (B) dorsal view; (C) articular-surface view.

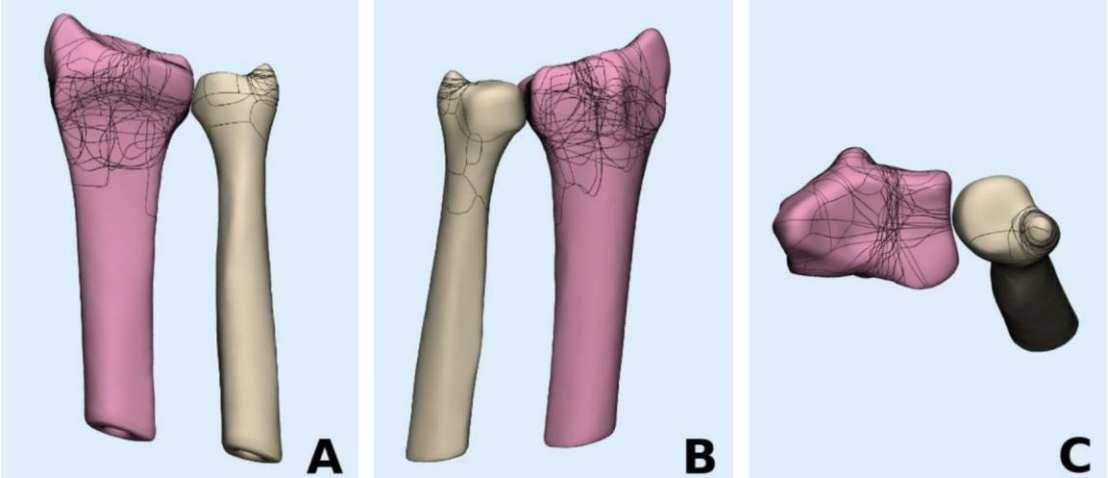


Figure 9. Fracture-line distribution map of 18 RUAL type III fractures. (A) Volar view; (B) dorsal view; (C) articular-surface view.

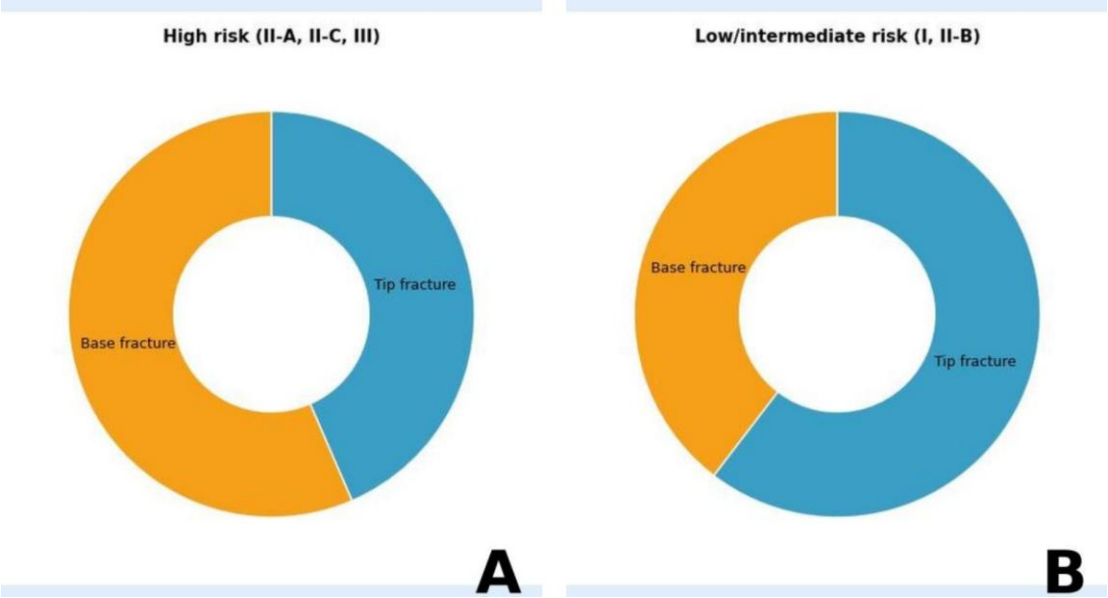


Figure 10. Distribution of ulnar styloid fracture location in the morphologic high-risk and low/intermediate-risk groups. (A) High-risk group (types II-A, II-C, and III); (B) low/intermediate-risk group (types I and II-B).

Table 1 Comparison of Baseline Characteristics Across RUAL Types

Variable	Type I (n=100)	Type II (n=115)	Type III (n=18)	Statistic	P
Sex, n (%)				χ^2=1.084	0.582
Male	37 (37.0)	45 (39.1)	9 (50.0)		
Female	63 (63.0)	70 (60.9)	9 (50.0)		
Age, years, mean ± SD	58.9 ± 11.5	59.5 ± 12.1	59.3 ± 11.9	F=0.069	0.933
Mechanism of injury, n (%)				Exact test	0.610
Low-energy injury	89 (89.0)	99 (86.1)	17 (94.4)		
High-energy injury	11 (11.0)	16 (13.9)	1 (5.6)		

Sex was analyzed using the Pearson chi-square test; age using one-way analysis of variance; and mechanism of injury using the two-sided Fisher–Freeman–Halton exact test.

Table 2 Distribution of Ulnar Styloid Fracture Location Across RUAL Subtypes

RUAL subtype	n	Tip fracture, n (%)	Base fracture, n (%)	χ^2	P
I-Ext	34	20 (58.8)	14 (41.2)		
I-Int	66	39 (59.1)	27 (40.9)		
II-A	16	6 (37.5)	10 (62.5)		
II-B	87	54 (62.1)	33 (37.9)		
II-C	12	5 (41.7)	7 (58.3)		
Type III	18	9 (50.0)	9 (50.0)		
Total	233	133 (57.1)	100 (42.9)	5.071	0.407

Percentages are within-subtype proportions. The overall comparison was performed using the Pearson chi-square test (df=5).

Table 3 Comparison of Ulnar Styloid Fracture Location Across the Three Major RUAL Types

RUAL type	n	Tip fracture, n (%)	Base fracture, n (%)	χ^2	P
Type I (I-Ext + I-Int)	100	59 (59.0)	41 (41.0)		
Type II (II-A + II-B + II-C)	115	65 (56.5)	50 (43.5)		
Type III	18	9 (50.0)	9 (50.0)		
Total	233	133 (57.1)	100 (42.9)	0.533	0.766

Percentages are within-type proportions. The Pearson chi-square test was used (df=2).

Table 4 Association Between Exploratory Risk Grouping and Ulnar Styloid Fracture Location

Risk group	n	Tip fracture, n (%)	Base fracture, n (%)	OR (95% CI)	χ^2	P
High-risk group (II-A, II-C, III)	46	20 (43.5)	26 (56.5)	1.99 (1.03–3.81)	4.329	0.037
Low/intermediate-risk group (I, II-B)	187	113 (60.4)	74 (39.6)	1.00 (reference)		

OR, denotes the odds ratio for an ulnar styloid base fracture. Pearson chi-square P=0.037; two-sided Fisher's exact P=0.046. This pooled risk analysis was exploratory and was not adjusted for multiple comparisons.

Table 5. Interobserver and Intraobserver Reliability of the RUAL Classification

Reliability assessment	n	Exact agreement, n (%)	κ (95% CI)	Z	P
Interobserver (round 1)	80	59 (73.8)	0.631 (0.496–0.765)	10.666	<0.001
Interobserver (round 2)	80	56 (70.0)	0.570 (0.424–0.717)	9.401	<0.001
Intraobserver (observer 1)	80	75 (93.8)	0.909 (0.831–0.986)	14.498	<0.001
Intraobserver (observer 2)	80	70 (87.5)	0.826 (0.726–0.927)	14.018	<0.001

κ denotes unweighted Cohen's kappa. The 95% CIs were calculated using large-sample asymptotic standard errors.